INVITED PAPER

LTE-ADVANCED: NEXT-GENERATION WIRELESS BROADBAND TECHNOLOGY

AMITAVA GHOSH, RAPEEPAT RATASUK, BISHWARUP MONDAL, NITIN MANGALVEDHE, AND TIM THOMAS, MOTOROLA INC.

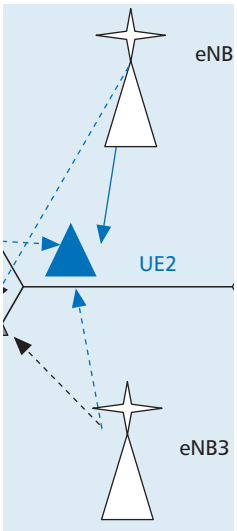

LTE-Advanced (also known as LTE Release 10) significantly enhances the existing LTE Release 8 and supports much higher peak rates, higher throughput and coverage and lower latencies resulting in a better user experience.

ABSTRACT

LTE Release 8 is one of the primary broadband technologies based on OFDM, which is currently being commercialized. LTE Release 8, which is mainly deployed in a macro/microcell layout, provides improved system capacity and coverage, high peak data rates, low latency, reduced operating costs, multi-antenna support, flexible bandwidth operation and seamless integration with existing systems. LTE-Advanced (also known as LTE Release 10) significantly enhances the existing LTE Release 8 and supports much higher peak rates, higher throughput and coverage, and lower latencies, resulting in a better user experience. Additionally, LTE Release 10 will support heterogeneous deployments where low-power nodes comprising picocells, femtocells, relays, remote radio heads, and so on are placed in a macrocell layout. The LTE-Advanced features enable one to meet or exceed IMT-Advanced requirements. It may also be noted that LTE Release 9 provides some minor enhancement to LTE Release 8 with respect to the air interface, and includes features like dual-layer beamforming and time-difference-of-arrival-based location techniques. In this article an overview of the techniques being considered for LTE Release 10 (aka LTE-Advanced) is discussed. This includes bandwidth extension via carrier aggregation to support deployment bandwidths up to 100 MHz, downlink spatial multiplexing including single-cell multi-user multiple-input multiple-output transmission and coordinated multi point transmission, uplink spatial multiplexing including extension to four-layer MIMO, and heterogeneous networks with emphasis on Type 1 and Type 2 relays. Finally, the performance of LTE-Advanced using IMT-A scenarios is presented and compared against IMT-A targets for full buffer and bursty traffic model.

INTRODUCTION

Universal Mobile Telecommunications System (UMTS) Long Term Evolution (LTE) Release 8 provides high peak data rates of 300 Mb/s on the downlink and 75 Mb/s on the uplink for a 20 MHz bandwidth, and allows flexible bandwidth operation of up to 20 MHz. Currently, enhancements are being studied to provide substantial improvements to LTE Release 8, allowing it to meet or exceed International Mobile Telecommunications-Advanced (IMT-A) requirements [1]. These enhancements are being considered as part of LTE-Advanced (LTE-A, also known as LTE Release 10), which includes carrier aggregation, advanced uplink (UL) and downlink (DL) spatial multiplexing, DL coordinated multipoint (CoMP) transmission, and heterogeneous networks with special emphasis on Type 1 and Type 2 relays.

This article provides an overview of the technologies being considered for LTE-A. This article is organized as follows. In the next section an overview of the LTE Release 8 physical layer (PHY) is provided. This is followed by an overview of evolved UMTS terrestrial radio access (E-UTRA) LTE-A requirements. In the following section a discussion on carrier aggregation is provided. We then provide an overview of DL and UL spatial multiplexing and fundamentals of DL CoMP design. We introduce the concept of heterogeneous networks, withy an emphasis on LTE relays. We compare the performance of LTE Release 8 and LTE-A in the context of IMT-A requirements. Finally, conclusions are drawn in the last section.

LTE RELEASE 8 PHY OVERVIEW

In LTE Release 8, orthogonal frequency-division multiplexing (OFDM) is the DL multiple access scheme, while single-carrier frequency-division multiple access (SC-FDMA) is the UL multiple access scheme. LTE Release 8 also supports scalable bandwidth up to 20 MHz, and uses DL/UL frequency selective and DL frequency diverse scheduling, respectively.

The DL subframe structure is common to both time-division duplex (TDD) and frequency-division duplex (FDD), and is shown in Fig. 1 for four transmit antennas using common reference symbols and a normal cyclic prefix. More than four transmit antennas can be supported using user-specific dedicated reference symbols. Each subframe consists of two slots of length 0.5 ms (7 OFDM symbols for normal cyclic prefix) with reference symbols located within each slot. DL control signaling is located in the first *n*

1536-1284/10/$25.00 © 2010 IEEE

OFDM symbols ($n \leq 3$) where n can be dynamically changed every subframe, followed by data transmission. The time-division multiplexing (TDM) structure between control and data enables micro-sleep to be implemented in the user equipment (UE, same as a mobile or a user). Micro-sleep allows the UE to turn off its power amplifier after determining that no data assignment is given to it in this subframe. This can significantly lower UE power consumption and extend its battery life. Each element in the time and frequency resource grid is called a resource element (RE). Each DL subframe contains reference signals, control information, and data transmission. The following physical channels provide DL control signaling: physical control format indicator channel (PCFICH), physical hybrid automatic repeat request (HARQ) indicator channel (PHICH), and physical DL control channel (PDCCH). Table 1 provides a brief overview of the purpose of these control channels. The DL and UL scheduling assignment transmitted on the PDCCH is addressed to a specific user, and contains control information needed for data reception and demodulation. Users are assigned data allocation in quanta of resource blocks (RBs), where an RB is defined as 12 REs by one slot.

In the UL, single-carrier frequency-division multiplexing (SC-FDM) is implemented via discrete Fourier transform spread OFDM (DFT-S-OFDM). DFT-S-OFDM has similar numerology to the OFDM transmission scheme used on the DL, with the main difference being that the constellation symbols are DFT precoded before mapping to the different subcarriers. The DFT precoding operation is performed to reduce the cubic metric (CM) of the signal, leading to higher maximum transmit power [2]. This CM reduction may be used to improve cell edge coverage and conserve UE battery life. Like the DL, frequency domain orthogonality is maintained among intracell users, which allows the enhanced Node B (eNB, where eNB is synonymous to base station in 3GPP lingo) the ability to efficiently manage the amount of interference seen at the base station. A block diagram for SC-FDMA implemented via DFT-S-OFDM is shown in Fig. 2.

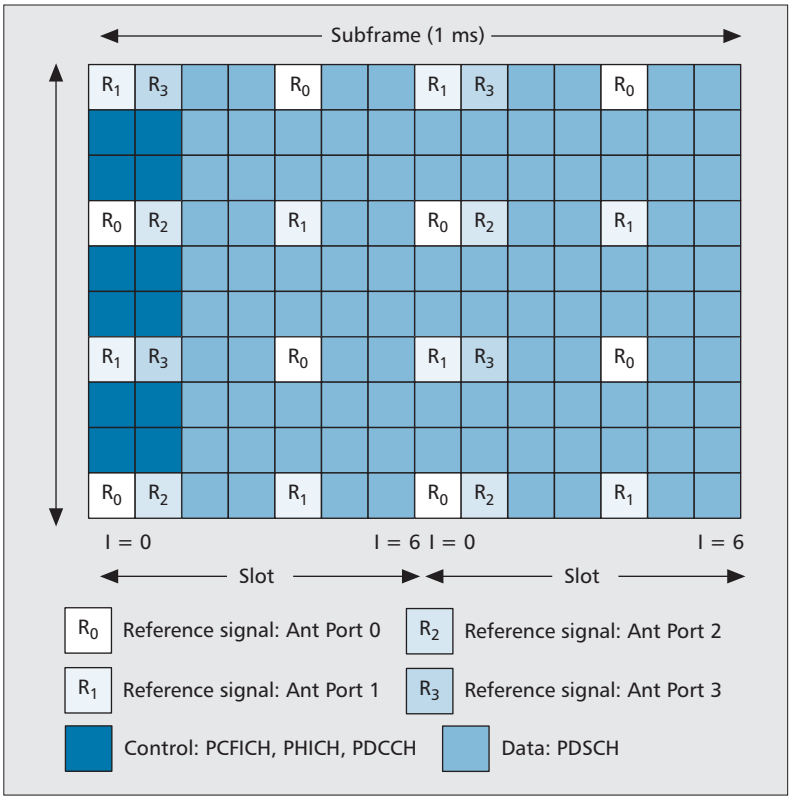

Figure 1. *Downlink subframe structure.*

The UL subframe structure is shown in Fig. 3 and is common for both FDD and TDD. Similar to the DL, each UL subframe consists of two slots of length 0.5 ms (7 DFT-S-OFDM symbols for normal cyclic prefix) with one reference symbol located within each slot. UL control signaling such as channel quality indication (CQI) and acknowledgment/negative acknowledgment (ACK/NACK) is located in the system band-edge. Two types of reference signals are supported on the UL: the demodulation reference

	Channel	Purpose
DL	PDSCH	Carry user data (DL)
	Physical broadcast channel (PBCH)	Carry broadcast information
	Physical multicast channel (PMCH)	Carry multicast services
	PCFICH	Indicate the size of the control region in number of OFDM symbols
	PHICH	Carry ACK/NACK associated with UL transmission
	PDCCH	Carry DL scheduling assignments and UL scheduling grants
UL	PUSCH	Carry user data (UL)
	PUCCH	Carry ACK/NACK associated with DL transmission, scheduling request, and feedback of DL channel quality and precoding vector
	Physical random access channel (PRACH)	Carry random access transmission

Table 1. *Physical channels in LTE.*

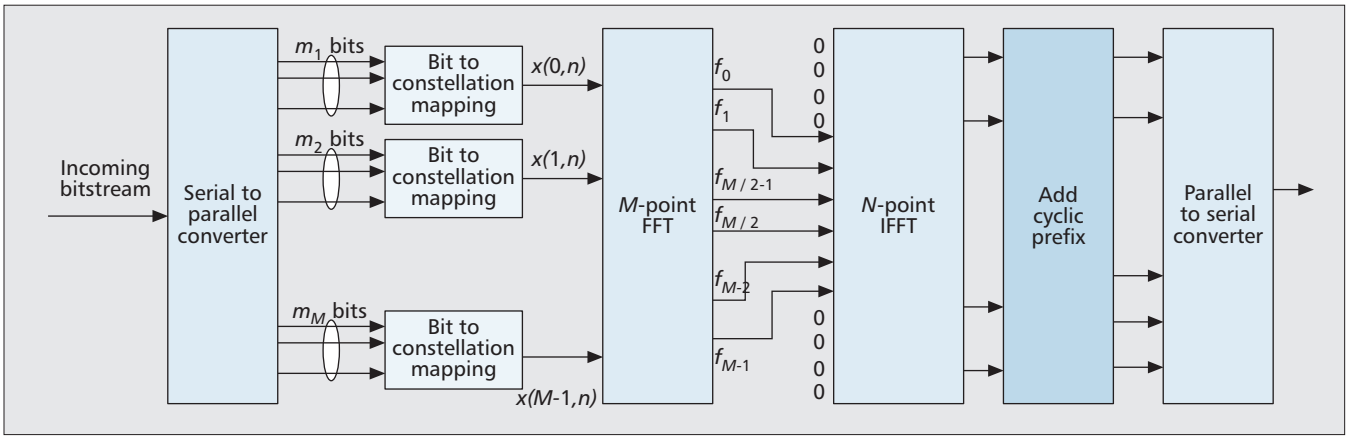

Figure 2. *Block diagram for SC-FDMA.*

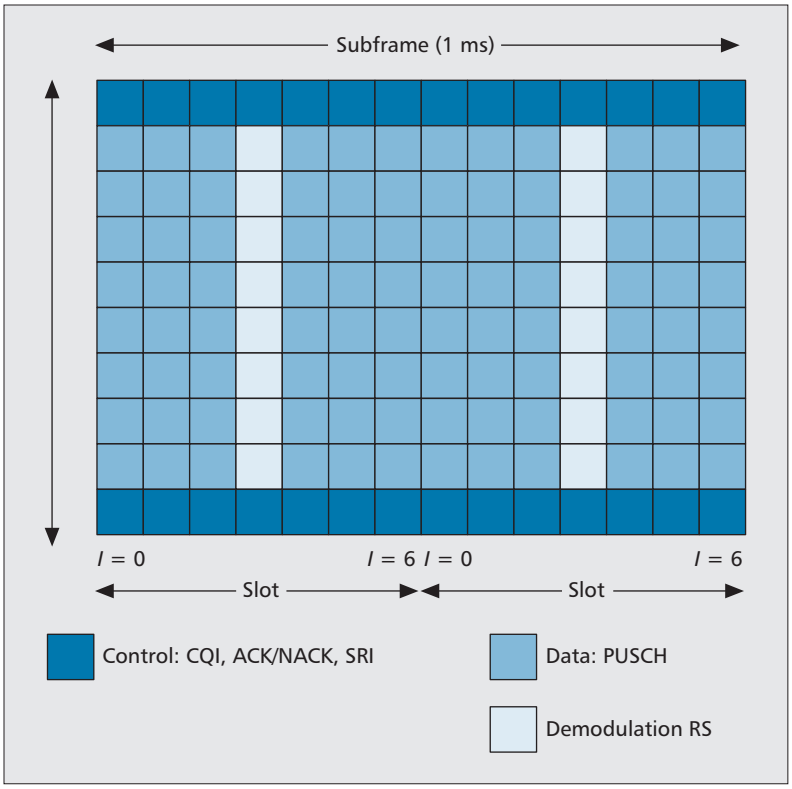

Figure 3. *Uplink subframe structure.*

Environments	DL LTE-A targets		UL LTE-A targets	
	Sector (b/s/Hz)	Cell edge (b/s/Hz)	Sector (b/s/Hz)	Cell edge (b/s/Hz)
Indoor	3	0.1	2.25	0.07
Microcellular	2.6	0.075	1.80	0.05
Base coverage urban	2.2	0.06	1.4	0.03
High speed	1.1	0.04	0.7	0.015
Peak spectral efficiency	15		6.75	

Table 2. *LTE-A targets for full buffer traffic.*

signal, used for channel estimation and demodulation of UL data or control, and the sounding reference signal, used for UL frequency selective scheduling and dedicated-reference-symbol-based beamforming on the DL. Currently, only one transmit antenna is supported at the UE.

Table 1 summarizes the available DL and UL physical channels and their purpose.

LTE-A Requirements

LTE-A is the evolutionary path from LTE Release 8. The LTE-A technology should be able to satisfy the IMT-A system requirements specified in [3]: "IMT-A systems are mobile systems that include the new capabilities of IMT that go beyond those of IMT-2000. Such systems provide access to a wide range of telecommunication services including advanced mobile services, supported by mobile and fixed networks, which are increasingly packet-based." As shown in this article, all of the IMT-A requirements cannot be fulfilled by LTE Release 8 and require technology beyond Release 8. As such, LTE-A is designed to meet and exceed these IMT-A requirements as summarized in Table 2. These requirements are met using a variety of techniques, including:

- Carrier aggregation
- DL spatial multiplexing using up to eight-layer multiple-input multiple-output (MIMO)
- DL intracell CoMP transmission and reception
- UL Spatial Multiplexing using four-layer MIMO

In addition to the improvement in spectral efficiency, substantial reduction in latency is also targeted. The goals are to reduce the transition time from idle to connected mode from 100 ms in LTE to less than 50 ms in LTE-A. Similarly, the transition from dormant to active should be reduced from 50 ms in LTE to less than 10 ms in LTE-A.

In LTE-A capacity and coverage enhancement can also be achieved using a heterogeneous network, which is a collection of low-power nodes distributed across a macrocell (homogeneous) network. There are various types of low-power nodes including microcells, picocells, femtocells, and relays. These low-power nodes are deployed in various environments

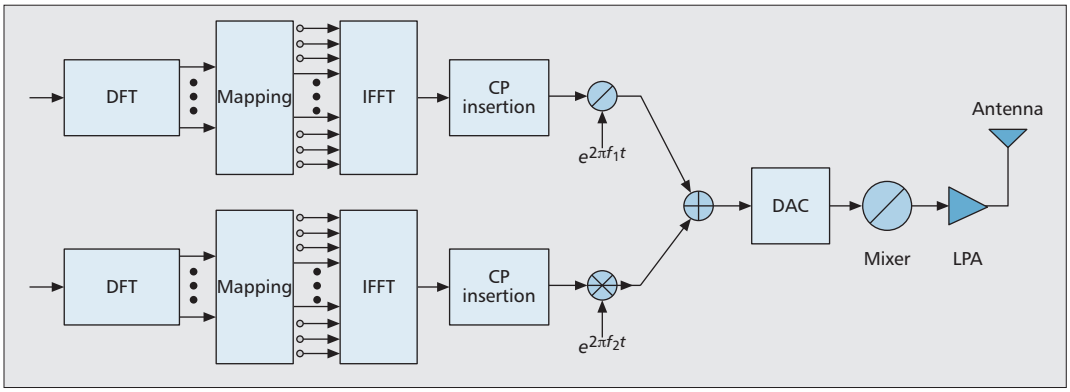

Figure 4. *Transmitter block diagram for uplink carrier aggregation.*

including hot spots, homes, enterprise environments, and low geometry locations to improve the overall capacity and coverage of the system.

Carrier Aggregation

Bandwidth extension in LTE-A is supported via carrier aggregation. Carrier aggregation allows deployment bandwidths of up to 100 MHz, enabling peak target data rates in excess of 1 Gb/s in the DL and 500 Mb/s in the UL to be achieved. In addition, it can be used to effectively support different component carrier types that may be deployed in heterogeneous networks. Carrier aggregation is attractive because it allows operators to deploy a system with extended bandwidth by aggregating several smaller component carriers while providing backward compatibility to legacy users. Three different types of component carriers are envisioned:

- **Backward-compatible carrier**: All LTE UE can access this type of carrier regardless of the supported release. In this case all of the current LTE features must be supported.
- **Non-backward-compatible carrier**: Only LTE-A UEs can access this type of carrier. This carrier may support advanced features such as control-less operations or the anchor-carrier concept not available to LTE UE.
- **Extension carrier**: This type of carrier operates as an extension of another carrier. It may be used, for example, to provide services to home eNBs in the presence of high interference from the macrocell. UE can only access this type of carrier as part of a carrier aggregation set. The extension carrier is addressed using a separate PDCCH and uses a separate HARQ process.

Three possible aggregation scenarios are possible: contiguous aggregation of component carriers in a single band, non-contiguous aggregation of component carriers in a single band, and non-contiguous aggregation of component carriers over multiple bands. Up to five component carriers may be aggregated together, providing a maximum bandwidth of 100 MHz. Under the current PHY specifications, the peak DL data rate for a 20 MHz system bandwidth is 150.752 Mb/s with two-layer spatial multiplexing and 299.552 Mb/s with four-layer spatial multiplexing. With carrier aggregation, these peak rates will scale linearly with the number of carriers. For instance, with carrier aggregation of 5 × 20 MHz carriers in the DL, a peak theoretical DL data rate of 1.5 Gb/s can be achieved without any additional features. In the UL a peak data rate of 75.376 Mb/s is currently possible. With carrier aggregation, a peak UL rate of 376.88 Mb/s is theoretically possible. A peak UL data rate in excess of 500 Mb/s can then be achieved with additional enhancements such as UL spatial multiplexing.

Prioritized deployment scenarios have been defined in [4] based on preferences provided by leading network operators. Illustrative examples include:

- UL: 40 MHz (20 + 20 MHz, 3.5 GHz), DL: 80 MHz (2 × 20 + 2 × 20 MHz, 3.5 GHz), FDD
- UL: 100 MHz, DL: 100 MHz (5 × 20 MHz, 3.5 GHz), TDD

Note that since non-contiguous multiband aggregation is possible, coverage and performance can be different across the aggregated component carriers. In addition, UE may be assigned different UL and DL component carrier sets that are subsets of the system configuration. For example, the cell may be configured to support UL: 40 MHz, DL: 80 MHz, while UE is configured to support on UL: 20 MHz, DL: 40 MHz. Different users within the cell may be configured differently, providing great implementation flexibility. This flexibility allows for efficient support of techniques such as load balancing, interference coordination, quality of service (QoS) management, and power control. In addition, different UE bandwidth capability classes and heterogeneous networks can also be supported. This flexibility, however, requires robust control channel design to support all possible configurations. For instance, with asymmetric carrier aggregation, some carriers are missing their counterparts which presents a challenge because pair-wise operational support (e.g., ACKs) are necessary for FDD. As a result, some carriers must be configured to support more than one counterpart.

UE Implementation

SC-FDMA using DFT-S-OFDM is the PHY access scheme in the UL. With carrier aggregation, N × SC-FDMA, which is conceptually analogous to parallel SC-FDMA transmitters is used. In this case N DFT-inverse fast Fourier transform (IFFT) pairs are required to implement

Bandwidth extension in LTE-A is supported via carrier aggregation. Carrier aggregation allows deployment bandwidths of up to 100 MHz, enabling peak target data rates in excess of 1 Gb/s in the DL and 500 Mb/s in the UL to be achieved.

Number of component carriers (*N*)	*N* × SC-FDMA			OFDMA
	QPSK	16-QAM	64-QAM	
1	1.2	2.2	2.3	4.0
2	2.6	3.0	3.2	
5	3.4	3.6	3.7	

Table 3. *Cubic metric comparison for* N × *SC-FDMA.*

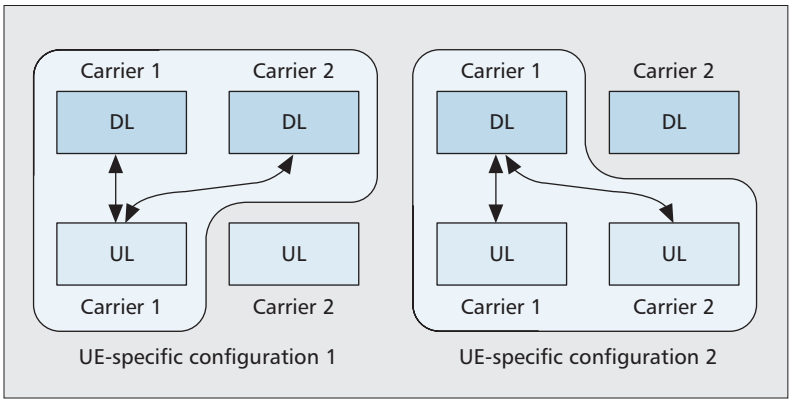

Figure 5. *Example of carrier aggregation configurations.*

carrier aggregation in the UL [5]. A block diagram of the UL demonstrating $N \times$ SC-FDMA for $N = 2$ is shown in Fig. 4. One potential issue with carrier aggregation is the limitation on the UE's transmission power. As a result, for FDD it is expected that two component carriers supporting aggregated bandwidth of 40 MHz may be the most practical scenario. For TDD, however, up to 100 MHz must be supported based on the DL bandwidth.

With carrier aggregation, the single carrier property in the UL is no longer preserved when transmitting on multiple carriers. As a result, the cubic metric (defined in [6] as the cubic power of the signal of interest compared to a reference signal) increases, which requires a larger backoff in the power amplifier, thereby reducing the maximum transmit power at the UE. An illustrative comparison is shown in Table 3 for different numbers of component carriers. For example, the cubic metric increases from 2.2 to 3.0 dB when the UE is transmitting using 16-quadrature amplitude modulation (QAM) on two simultaneous component carriers. This substantial increase in cubic metric has the effect of reducing the coverage when carrier aggregation is used, although it can be seen that the cubic metric is generally still less than that for orthogonal frequency-division multiple access (OFDMA, note that results for OFDMA are independent of modulation). In addition, the increase is most significant in going from one to two simultaneous component carriers, and only increases gradually as more carriers are used. It should be noted that since multicarrier transmission will usually be used for UE in good channel conditions, there should be no loss of coverage for those users. On the other hand, users at the cell edge will most likely be scheduled only on a single carrier. There is no difference in cubic metric in this case, and coverage may actually be improved since the eNB has the ability to dynamically assign users to the best UL carrier.

Data Transmission and Control Signaling

At the data layer, each component carrier operates independently with a separate data stream that is aggregated or segmented at the medium access control (MAC) layer. This MAC-PHY interface provides support for carrier aggregation with minimal changes to the PHY specifications. In this case separate HARQ processing and associated control signaling is required for each of the component carriers. This allows separate link adaptation and MIMO support for each carrier, which should improve throughput since each data transmission can be independently matched to channel conditions on each carrier. As a result, data processing at the PHY can be thought of as independent per carrier.

Control signaling serves several main purposes in LTE: to provide signaling related to scheduling assignments, to provide acknowledgment in response to data transmission, to provide channel state feedback information, and to provide power control information. To support carrier aggregation, these functions must be extended to support multiple component carriers. It should be noted that, in general, the principle is to extend the LTE design to multiple carriers when possible.

In the DL three control channels are presented: the PDCCH, used for scheduling assignments and power control; the PCFICH, used to indicate the size of the DL control region; and the PHICH, used to provide acknowledgment in response to UL data transmission.

For the PDCCH, a separate scheduling grant has been adopted where each grant addresses one carrier. To allow for scheduling flexibility, each grant will contain a carrier indication field (CIF) to indicate to which carrier the grant applies, which thus allows the reuse of existing LTE scheduling grant formats with only the addition of the CIF. By using a separate grant structure, the eNB has the ability to schedule different grant formats to the same UE in different component carriers, and perform dynamic grant load balancing and interference coordination among the component carriers on a subframe basis.

For the PCFICH, the channel is expected to be configured independently for each component carrier. A UE will therefore independently decode the PCFICH and determine the data boundary as in LTE. In the case of a PDCCH-less carrier (e.g., extension carrier in a heterogeneous network), this would be known to the user and no special handling is necessary.

Since separate HARQ processing is used, associated control signaling will be required for each of the component carriers. In addition, LTE-A UE can be configured with UE-specific UL/DL carrier aggregation configurations that are a subset of the system configuration shown in Fig. 5. The ACK is transmitted on the same DL carrier as the UL scheduling assignment, which allows many simultaneous UE-specific

configurations to be supported. This feature solves the issue with UL-heavy aggregation and also does not require an explicit DL-UL pairing relationship to be defined. Although this will require the eNB to manage the PHICH, it will be similar to the PDCCH management that will also be required.

UL control signaling carries ACKs for the DL data transmission and channel state feedback (e.g., CQI, precoding matrix indication [PMI], or rank indication [RI]). In the UL, the simplest possible approach is to support an individual UL control channel per carrier based on the Release 8 structure. Thus, each UL control channel may be configured independently to support one DL-UL carrier pair. In the case of asymmetric carrier aggregation, additional UL control signaling (ACK/NACK and CQI) may be configured to support multiple DL carriers on a single UL carrier. One concern for the UL is the limited transmission power available to the UE. As a result, it may not be possible to transmit feedback or acknowledgments from many component carriers simultaneously. In this case it is possible that some form of control information multiplexing such as ACK/NACK bundling may be used. In addition to carrier aggregation, within the same carrier, UE has the ability to simultaneously transmit both the physical uplink shared channel (PUSCH) and physical uplink control channel (PUCCH). With carrier aggregation in addition to simultaneous PUSCH and PUCCH transmission, the total cumulative power the UE is allowed to transmit across all component carriers should not exceed the maximum UE power. Under a transmit power limitation, power reduction based on per-channel scaling is used where scaling factors are used such that power reduction is first performed on the PUSCH.

DL/UL Spatial Multiplexing and DL CoMP

The DL MIMO transmission schemes already supported in LTE Release 8 include transmit-diversity and open-loop and closed-loop spatial multiplexing with up to four layers. These MIMO schemes are supported by common reference signals (common pilots) broadcast from an eNB. Codebook-based precoding is used to support closed-loop spatial multiplexing. In addition, a single layer of a UE-specific reference signal (also known as dedicated pilots) is available that may be used for beamforming. The UE-specific reference signal enables single-layer beamforming in TDD scenarios where the DL spatial channel information may be obtained at the base station using channel reciprocity. A multi-user MIMO (MU-MIMO) transmission scheme may also be applied based on codebook feedback. However, the performance of the MU-MIMO scheme is limited by coarse quantization (using codebook) and the lack of support for cross-talk suppression at the UE. As a result, MU-MIMO in Release 8 does not provide any performance gains compared to SU-MIMO. Fortunately, LTE-A will fix the MU-MIMO performance, as we will see.

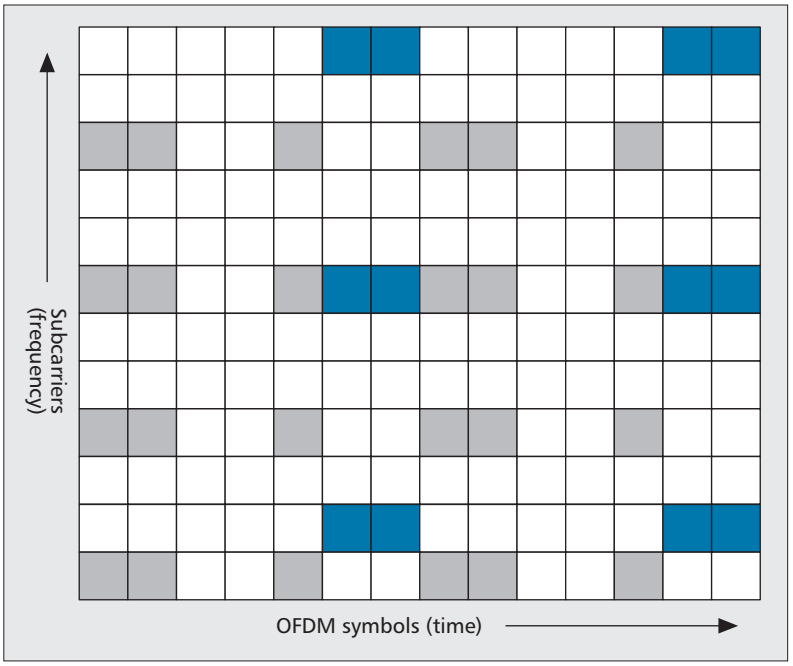

Figure 6. *Two layers of UE-specific reference signals (dark blue) separated by code in a resource block. The shaded resources indicate common reference signals for four antenna ports present in Release 8.*

The performance of DL and UL transmission in LTE Releases 9 and 10 will be enhanced by the following features [7]:

- Enhanced single-cell DL MU-MIMO support
- Extension to eight-layer DL spatial multiplexing
- DL CoMP support
- Extension to four-layer UL spatial multiplexing

Some of the above features are necessary to meet the IMT-A requirements as is shown later.

Enhanced Single Cell DL MU-MIMO Support

In LTE Release 9 two layers of orthogonal UE-specific reference signals have been introduced, as shown in Fig. 6. This enables an eNB to transmit two layers of data to a UE set using spatial multiplexing in a closed-loop mode by constructing antenna weights using channel reciprocity. Additionally, this enables an eNB to transmit two layers of data to two UE sets (one layer each) using the same time-frequency resource in MU-MIMO fashion. Switching between single- and dual-layer transmission to a single UE set, as well as between SU-MIMO and MU-MIMO is supported in a dynamic fashion. The control signaling overhead for supporting dynamic and transparent MU-MIMO transmission is small because UE is not explicitly informed of the presence of co-scheduled UE, for the purposes of feedback or demodulation. The two layers of UE-specific reference signals are overlaid on top of each other (separated by a length 2 orthogonal cover code) and a UE, after subtracting out its channel estimate, may estimate a covariance matrix representing the combined interference from a co-scheduled UE and outer cell transmissions. This feature can be used by a receiver to significantly suppress the interference due to MU-MIMO. The MU-MIMO enhancements in

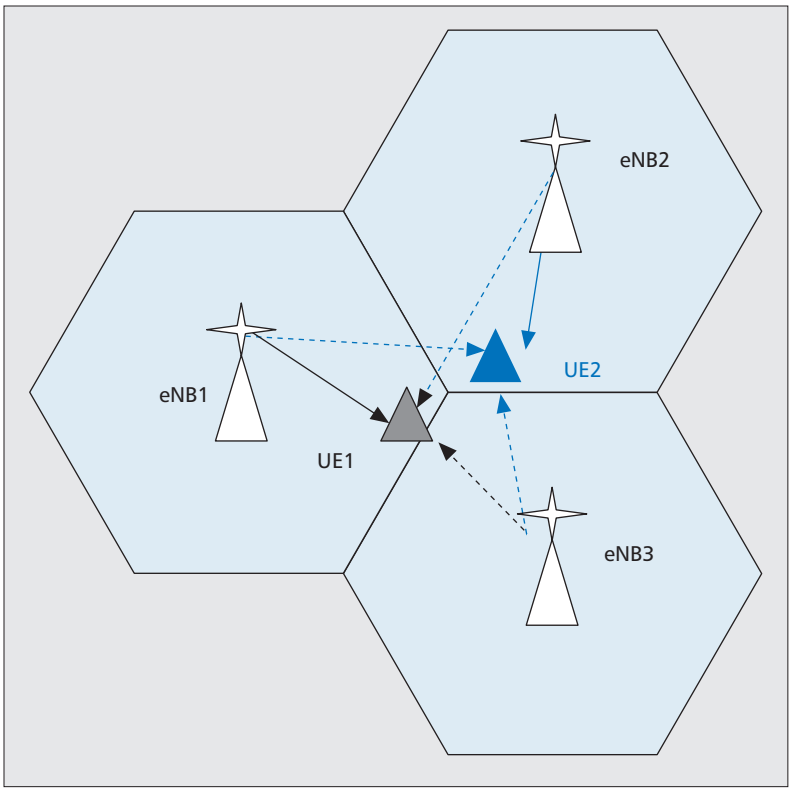

Figure 7. *A CoMP framework for DL transmission where eNB1, eNB2, and eNB3 can coordinate and create a multipoint transmission to UE1 and UE2.*

Release 9 provide substantial gains in sector throughput when the eNB is able to form transmit beams using reciprocity-based techniques. Note that with channel reciprocity based MU-MIMO, there is no restriction on the number of transmit antennas that can be employed at the eNB. In addition, up to four layers of quasi-orthogonal UE-specific reference signals is available for MU-MIMO enabling co-scheduling of up to four UE sets in the same time-frequency resource.

In Release 10 an enhancement to provide high-resolution spatial channel feedback is being considered to support MU-MIMO in cases where channel reciprocity is not reliable.

Extension to 8-Layer DL Spatial Multiplexing

The extension to eight-layer spatial multiplexing is aimed at improving the DL peak throughput of a Release 10 system employing eight or more transmit antennas. Accordingly, eight layers of UE-specific reference signals will be introduced for demodulation. Since the density of UE-specific reference signals can be adapted based on the number of layers of data transmission and the size of the resource allocation, it is more economical to use UE-specific reference signals compared to common reference signals for supporting higher-order spatial multiplexing. The maximum number of transport blocks transmitted over eight layers will remain two with support for separate modulation and coding schemes (MCSs) and separate HARQ ACKs.

In order to support feedback of channel quality, choice of frequency bands, or channel spatial information (e.g., codebook) for up to eight layers, additional reference signals will be broadcast from an eNB. These channel state information reference signals (CSI-RSs), however, will not be used for demodulation, and will be designed to be sparse in time and frequency with an overhead of around 1 percent or less. The CSI-RS design will support up to eight transmit antennas and will potentially enable UE at the cell edge to measure CSI-RSs transmitted from adjacent cells (for CoMP support). The power, density, and placement of CSI-RSs will have to be designed carefully as they may interfere with the data transmissions of a Release 8 or 9 user in the same subframe.

DL CoMP Support

The motivation of the CoMP feature is to provide air interface support to enable cooperation among eNBs that may or may not be collocated. Multiple eNBs may cooperate to determine the scheduling, transmission parameters, and transmit antenna weights for a particular UE. This cooperation will depend on a high-capacity backhaul link being available between eNBs. Closed loop beamforming or precoding-based transmissions will be supported in CoMP. This framework is depicted in Fig. 7, where three eNBs may coordinate to create a multipoint transmission to UE1 (served by eNB1) and UE2 (served by eNB2). The objective of CoMP is to reduce interference for a UE set in the network that is close to multiple eNBs and therefore experiences an interference-limited environment. The interference to these UE sets may be reduced and can be predicted if there is some coordination between the interfering eNBs and the serving eNB. The control overhead, feedback methods, and scheduling restrictions necessary to enable CoMP are under investigation. Within the timeframe of Release 10 a standardized interface of direct communication between two eNBs (i.e., the X2-interface) will not be redefined. Therefore, the coordination needed for CoMP will depend on proprietary interfaces that may easily be possible for intersector coordination. A similar framework for eNB cooperation for UL transmission is also under study.

Extension to Four-Layer UL Spatial Multiplexing

It is envisioned that Release 10 compatible UE may support up to four transmit antennas, and the extension to four-layer spatial multiplexing is targeted to improve the UL peak rate in such cases. As in Release 8, the UL transmission scheme for Release 10 will be DFT-precoded OFDM that will retain the single carrier property and restrict the peak-to-average power ratio (PAPR) or the cubic metric [t] of the UL waveform to a low value. Open-loop and closed-loop spatial multiplexing will be supported, and in the case of closed-loop operation, codebook-based precoding will be used. In contrast to the DL, the transmission schemes in the UL are optimized to preserve the single-carrier property or reduce PAPR/cubic metric. As an example, layer

shifting is a mechanism introduced to transmit data from multiple layers through a given antenna while maintaining single-carrier properties. Layer shifting has been proposed to provide robustness to spatial multiplexing against antenna gain imbalances and CQI mismatches due to velocity. Codebook designs are also being studied to enable precoded transmission with low PAPR/cubic metric. In addition, the codebook will also provide the capability to turn off certain antennas (for power saving) at the instruction of an eNB.

Heterogeneous Networks

In heterogeneous networks low-power nodes are distributed throughout macrocell networks. Low-power nodes can be micro eNBs, pico eNBs, home eNBs (for femtocells), relays, and distributed antenna systems (DASs), the latter of which may employ remote radio head (RRH) cells. These types of cells operate in low-geometry environments and produce high interference conditions. Such deployments enable optimization of network performance at relatively low cost. The various types of heterogeneous deployments are summarized in Fig. 8, and the definitions of the various low power nodes are summarized in Table 4 [7, 8]. In addition to CoMP, intercell interference coordination (ICIC) techniques can play a critical role in obtaining good performance within heterogeneous deployments.

In this article one of the components of heterogeneous networks, relay nodes (RNs), is discussed in detail. Repeaters can also offer coverage extension for eNBs by amplifying and forwarding received waveforms, but suffer from the following disadvantages: they cannot distinguish between signals and interference/noise, and RF isolation is a big issue. Relays typically yield performance improvement by providing higher throughputs to UE that would otherwise be located in poor geometry locations with respect to the macrocell sites. There are two types of relays being discussed in the context of 3GPP standards, Type 1 and Type 2 relays. Type 1 and Type 2 relays have the following characteristics:

- *Type 1*:
  - –A relay cell should have its own physical cell ID and transmit its own synchronization channels, reference symbols, and so on, and will be distinct from the donor cell.
  - –The UE should receive scheduling information and HARQ feedback directly from the RN and send its control channels (SR/CQI/ACK) to the RN.
  - –The RN appears as a Release 8 eNB to Release 8 UE.
- *Type 2*:
  - –The RN does not have a separate Physical Cell ID and thus would not create any new cells.
  - –It is transparent to Release 8 UE; Release 8 UE is not aware of its presence.
  - –It can transmit physical downlink shared channel (PDSCH) but does not transmit CRS and PDCCH.

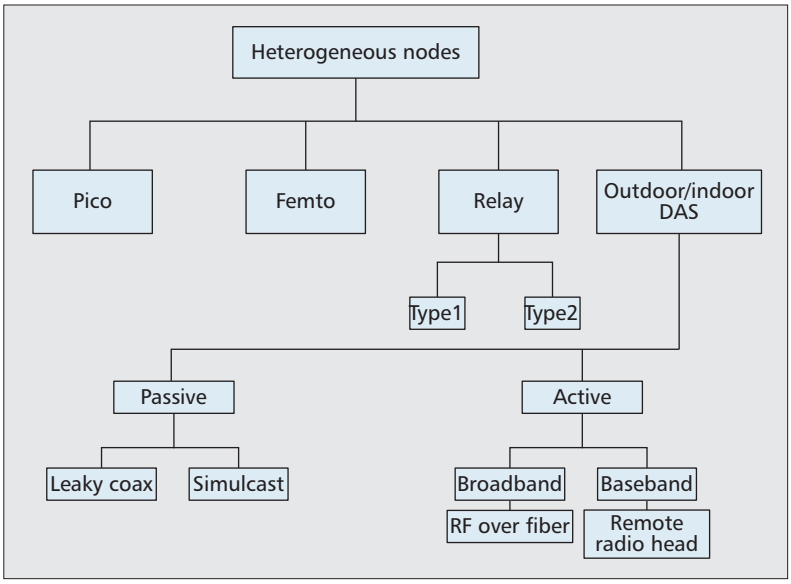

Figure 8. *Classification of heterogeneous deployments.*

The RNs are connected to the radio access network (RAN) via a donor macrocell. Two types of backhaul connections can be supported: in-band (IB), where the eNB-to-relay link shares the same band with direct eNB-to-UE links within a cell, and out-of-band (OOB), where the eNB-to-relay link does not share the same band with direct eNB-to-UE links .

For the IB scenario, backhaul traffic is facilitated by configuring certain subframes as multicast broadcast single-frequency network (MBSFN) subframes in the relay cell. These subframes are then used by a relay node to receive DL backhaul traffic from its donor eNB. This

Type of nodes	LPA power	# of Tx/Rx antennas	Backhaul characteristics	Comments
Micro eNBs	30 dBm–10 MHz carrier	2/2 or 4/4	X2	Open to all UE; placed outdoors
RRH nodes	30 dBm–10 MHz carrier	2/2 or 4/4	Several μs latency to macro	Open to all UE; placed indoors or outdoors
Pico eNBs	30 dBm–10 MHz carrier	2/2 or 4/4	X2	Open to all UE; placed indoors or outdoors
Home eNBs	20 dBm–10 MHz carrier	2/2 or 4/4	Home broadband	Closed subscriber group, placed indoors
Relays	30 dBm–10 MHz carrier	2/2 or 4/4	Wireless out-of-band or in-band	Open to all UE; placed outdoors

Table 4. *Characteristics of low power nodes.*

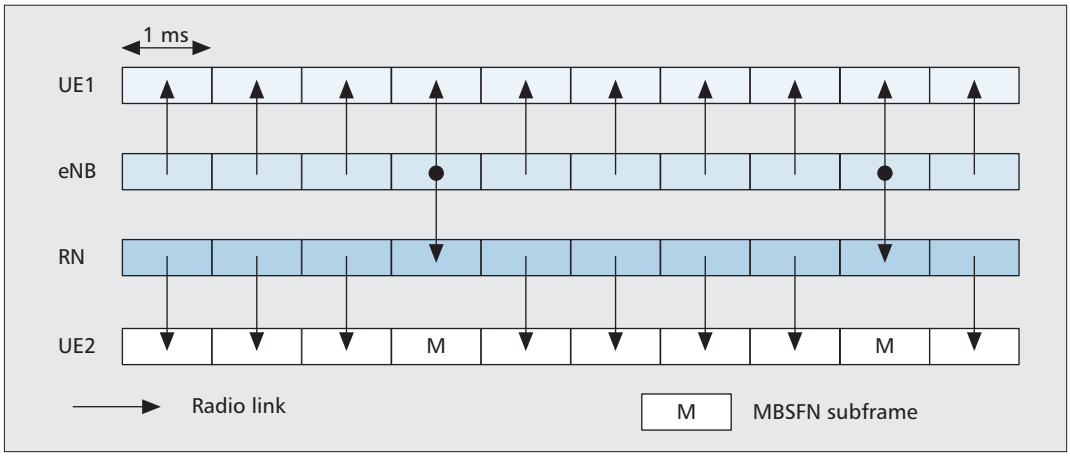

Figure 9. *Radio links and subframe utilization at different nodes in the network.*

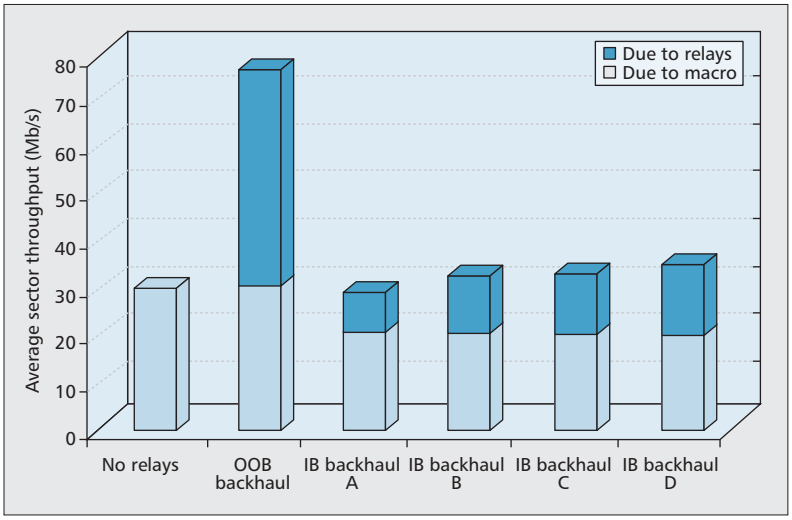

Figure 10. *Average sector throughput due to macro and relay cells for DS case 3 (one backhaul SFpF for in-band backhaul).*

configuration is illustrated in Fig. 9, where the utilization of subframes at eNBs, RNs, macrocell UE (UE1), and relay cell UE (UE2) is shown. The arrows show the direction of transmission for radio links in each subframe. Thus, subframes are normally used for access links; that is, DL transmission from an eNB or RN to its UE except during the MBSFN subframes, when UE in the relay cell does not receive data, whereas eNBs may transmit DL traffic to both RNs (i.e., backhaul traffic) as well as macrocell UE (access traffic). The set of such DL backhaul subframes is semi-statically assigned, whereas the set of UL backhaul subframes is either semi-statically assigned or implicitly derived from the DL backhaul subframes using the HARQ timing relationship. For simplicity, our simulation study assumes that the same DL backhaul subframe configuration is maintained throughout the network.

The DL subframe boundaries for the access and backhaul links are aligned at the RN while allowing an adjustment for RN transmit/receive switching. A new physical control channel, R-PDCCH, is defined for the eNB to assign backhaul resources to the RN. A set of physical RBs (PRBs) is semi-statically assigned for the transmission of the R-PDCCH. The actual resources used within these PRBs may vary dynamically between subframes. Furthermore, these resources may correspond to either the full set of OFDM symbols available for the backhaul link or a subset of them. The R-PDCCH is transmitted starting from an OFDM symbol within the subframe that is late enough so that the RN can receive it (i.e., such that the RN can complete transmission of its own PDCCH and switch to receive). The assignment of DL and UL backhaul resources on the R-PDCCH may be done either dynamically or semi-persistently. DL backhaul resources may be assigned for either the same subframe and/or a later subframe. UL resources may be assigned for one or more later subframes.

Four models are considered for the IB backhaul link. The models to be used for path loss, antennas, and lognormal shadowing on the access and backhaul links are described in [7]. The first path loss model is that of non-optimized relay site planning with a single omnidirectional antenna set at the RN. We refer to this model as backhaul A. The backhaul model for optimized relay site planning with a single omnidirectional antenna set is referred to herein as backhaul B. The next two models assume the presence of two antenna sets at the RN, an omnidirectional antenna set for the relay access links, and a directional antenna set for the backhaul link (i.e., for receiving DL data from the eNB). The backhaul model with a directional antenna and non-optimized relay site planning is called backhaul C. Finally, the model that combines a directional antenna with optimized relay site planning is referred to as backhaul D.

A two-ring, 19-macrocell, three-sectored site hexagonal grid system layout is simulated with dual-port UE receiver operation and assuming TU channels using cell wrap-around for two systems, each operating in a 10 MHz bandwidth, corresponding to deployment scenario (DS) cases 1 and 3. One thousand four hundred twenty-five UE sets are randomly dropped with uniform spatial probability density over the entire 57-cell network. For the results presented here, a deployment with 228 relays is considered. The relays are dropped randomly over the entire network with a uniform spatial distribution.

The number of in-band backhaul subframes per frame (SFpF) shared among all RNs in a sector is a parameter. By controlling the number of backhaul SFpF, the size of the backhaul pipe can be controlled (at the expense of the resources available for the macrocell access links). Note that this is the total number of subframes shared by all backhaul links in the sector. For IB backhaul, the scheduler of each RN is constrained to allocate resources to its UE only when the amount of data it has transferred to the UE does not exceed the amount of data the RN has received from the donor eNB. This constraint ensures that the relay-cell throughput does not exceed the corresponding backhaul throughput. For OOB backhaul simulations, it is assumed that the backhaul is ideal and unconstrained.

Sample results are provided in Figs. 10 and 11. In Fig. 10 the aggregate sector throughput for DS case 3 is shown as the sum of its two components: due to the macrocell and due to all RNs (when present) associated with a donor macrocell. Clearly, ideal OOB backhaul yields the best throughput performance since unlimited backhaul capacity is assumed to be freely available. With IB backhaul, backhaul D performs best, being aided by both optimized relay site planning and a directional antenna. Figure 11 demonstrates cell edge (5th percentile) throughput performance for DS case 1 without and with relays. Again, OOB backhaul exhibits the best performance. The variation of performance with the number of backhaul SFpF (S) is also illustrated for IB backhaul. The cell edge throughput increases with S for all backhaul models since relay-cell edge UE benefits from increasing backhaul capacity. However, different backhaul models benefit to different extents, and backhaul C exhibits marginally superior cell edge performance to that of other IB backhaul models. Ongoing efforts are examining the scenarios that will benefit from relays with emphasis on opti-

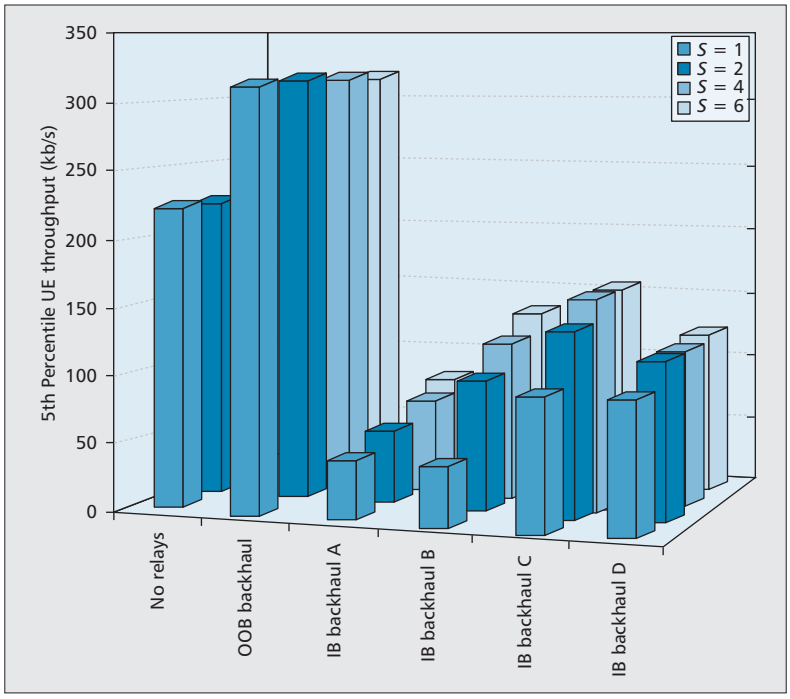

Figure 11. *5th percentile UE throughput for DS case 1 without and with relays (S: backhaul SFpF for in-band backhaul).*

Parameter	Value
Deployment scenarios	InH, UMi, UMa, RMa
Number of control symbols	3
Base station transmit antenna	2 and 4
Base station antenna configuration	Pair(s) of cross poles with 0.5λ
UE Rx antenna	2
UE Rx antenna configuration	0.5λ, v-pol
Channel estimation	Non-ideal
Receiver algorithm	MMSE
Precoding	Dynamic SU/MU-MIMO with zero-forcing beamformer
Feedback information	Ideal co-variance matrix, CQI
Feedback periodicity/delay	5 ms/2 ms
Frequency selective scheduling	Yes
Subband size	6 RB
Scheduling fairness	Proportional fair, fairness factor = 1.6

Table 5. *Main simulation assumptions.*

Deployment scenario		IMT-A req.	Ant. config.	
			2 × 2	4 × 2
InH	Cell spectral efficiency (b/s/Hz/cell)	2.250	4.360	—
	Cell edge user spectral efficiency (b/s/Hz)	0.070	0.146	—
UMi	Cell spectral efficiency (b/s/Hz/cell)	2.600	2.050	2.430
	Cell edge user spectral efficiency (b/s/Hz)	0.075	0.061	0.071
UMa	Cell spectral efficiency (b/s/Hz/cell)	2.200	1.150	1.560
	Cell edge user spectral efficiency (b/s/Hz)	0.060	0.022	0.032
RMa	Cell spectral efficiency (b/s/Hz/cell)	1.100	1.410	1.810
	Cell edge user spectral efficiency (b/s/Hz)	0.040	0.031	0.043

Table 6. *LTE Release 8 DL performance summary.*

Deployment scenario		IMT-A req.	4 × 2 linear array
UMi	Cell spectral efficiency (b/s/Hz/cell)	2.600	2.880
	Cell edge user spectral efficiency (b/s/Hz)	0.075	0.105
UMa	Cell spectral efficiency (b/s/Hz/cell)	2.200	2.480
	Cell edge user spectral efficiency (b/s/Hz)	0.060	0.063
RMa	Cell spectral efficiency (b/s/Hz/cell)	1.100	2.940
	Cell edge user spectral efficiency (b/s/Hz)	0.040	0.077

Table 7. *LTE-A DL performance summary.*

mization with respect to better distribution of users between macrocells and relay cells, and interference management schemes.

LTE-A Performance

Downlink

The simulations are based on the IMT-A evaluation document [9], and the simulation assumptions are outlined in Table 5. Downlink simulation results using LTE Release 8 features are shown in Table 6 for the base station antenna configuration shown in Table 5. Although the results shown in Table 5 are for an FDD deployment, results for TDD systems are similar in terms of spectral efficiency.

From the results, it is seen that IMT-A requirements can be met for indoor (InH) and rural macrocell (RMa) environments. This is especially true for the InH environment, where only a 2 × 2 antenna configuration is needed. However, DL performance for urban microcell (UMi) and urban macrocell (UMa) are below the IMT-A requirements. The shortfall is especially pronounced for the UMa environment, where approximately 70 percent of the sector and 60 percent of the cell edge requirements can be achieved.

Table 7 provides DL performance results using the LTE-A MIMO technique described earlier — enhanced single-cell DL MU-MIMO. From the table it is seen that the performance improves substantially in all cases and that the IMT-A requirements can be met in all environments.

Next, the DL performance using a different workload (bursty traffic model) is summarized. The bursty traffic model is important to characterize the dependency of the user data rate as a function of network load and user geometry. The characteristics of this model are as follows:

- Model users only for the duration of the file transfer.
- Users are randomly created and start file transfers in the simulated network at a certain rate according to a Poisson process.
- Data transfer users are modeled for the duration of the file transfer and then dropped from the simulation once the file data volume is transferred.
- For the period of the file transfer the application is assumed to download as quickly as the network allows.

In the simulation the UE arrival is random between 0 and 64 s with a total run time of 128 s. Statistics are collected between 16 and 64 s, and the file size used is 2 Mbytes. A new metric called *resource utilization* is defined which is given by the fraction of the total available air interface resources utilized for user-generated traffic (except for MU-MIMO or beamforming). In other words, it equals the average number of RBs used for user traffic over the duration of the simulation, divided by the number of RBs available to carry user traffic. The DL performance using 2 × 2 SU-MIMO with closely placed cross-pole antennas is summarized in Table 8. It may be observed from the table that the mean user data rate at 50 percent resource utilization (normal operating point) is around 11 Mb/s, while the 5 percent edge throughput is approximately 1.8 Mb/s.

Uplink

Uplink simulation results using LTE Release 8 features for two antenna configurations (1 × 4 and 1 × 8 linear arrays of vertically polarized elements with 0.5λ separation) under FDD systems are shown in Table 9. Frequency selective scheduling based on the proportional fair metric is used together with fractional UL power control. From the results, it is seen that with four receive antennas at the eNB, all IMT-A requirements can be met using the existing Release 8 functionality and 1 × 4 antenna configuration. With eight receive antennas, the cell spectral efficiency is significantly increased; therefore, more UL overhead can be accommodated. For instance, under the UMa scenario, the number of PUCCH RBs can be increased from 4 to 18 (36 percent control overhead) while still satisfying the IMT-A requirement. For UMi, the number of PUCCH RBs can be similarly increased from 4 to 16 RBs (32 percent control overhead). Note that the interference-over-thermal-noise ratio (IoT) in each case was constrained to be in the range of approximately 9–11 dB.

Although not shown here, results for TDD

Offered load	Served cell throughput	Mean user data rate	95% user data rate	50% user data rate	5% user data rate	Resource utilization	User outage
Mb/s	Mb/s	Mb/s	Mb/s	Mb/s	Mb/s	%	%
1	0.99	46.44	51.79	51.65	28.32	2.28	0.00
2	1.98	40.53	51.78	44.30	18.37	5.45	0.00
4	3.97	30.25	51.72	28.37	10.52	15.04	0.00
6	5.99	20.36	46.98	17.65	5.35	33.20	0.00
8	8.05	12.50	34.02	9.12	2.11	60.79	0.00
10	9.65	6.36	23.77	3.29	0.72	80.14	0.00
Full buffer	18.57	1.86	5.28	1.28	0.44	100.00	0.00

Table 8. *Bursty traffic performance with 2 × 2 SU-MIMO, UMi, 10 MHz.*

systems are similar in terms of spectral efficiency. In addition, performance under different antenna configurations, with 10λ separation and multiple pairs of cross-polarized antennas, was also similar (but slightly better in this case).

Finally, the performance of UL for the bursty traffic model is summarized in Table 10. It may be noted that the mean user data rate at 50 percent resource utilization is around 10 Mb/s, while the 5 percent edge throughput is approximately 1.5 Mb/s.

Conclusion

This article gives a brief overview and description of the concepts of the LTE-A features and the performance achievable using some of these features. It may be observed that requirements for IMT-A can be met using these advanced concepts. Finally, it may be noted that the work on LTE-A is still ongoing, and a follow-up to this article will be published at a later date.

Deployment scenario		IMT-A req.	Ant. config.	
			1 × 4	1 × 8
InH	Cell spectral efficiency (b/s/Hz/cell)	2.250	2.970	3.364
	Cell edge user spectral efficiency (b/s/Hz)	0.070	0.203	0.246
UMi	Cell spectral efficiency (b/s/Hz/cell)	1.800	1.904	2.413
	Cell edge user spectral efficiency (b/s/Hz)	0.050	0.057	0.074
UMa	Cell spectral efficiency (b/s/Hz/cell)	1.400	1.487	2.015
	Cell edge user spectral efficiency (b/s/Hz)	0.700	1.600	2.110
RMa	Cell spectral efficiency (b/s/Hz/cell)	1.100	1.410	1.810
	Cell edge user spectral efficiency (b/s/Hz)	0.015	0.054	0.072

Table 9. *LTE Release 8 UL performance summary.*

Offered load	Served cell throughput	Mean user data rate	95% user data rate	5% user data rate	10% user data rate	Resource utilization	User outage	Mean IoT	Stand. deviation IoT
Mb/s	Mb/s	Mb/s	Mb/s	Mb/s	Mb/s	%	%	dB	dB
1	1.03	17.13	22.97	5.64	7.61	7.3	0.1%	0.9	0.4
2	1.99	15.64	22.97	4.35	5.91	14.9	0.1%	1.8	2.8
4	3.98	12.71	22.93	2.46	3.59	34.9	0.2%	4.2	6.3
6	5.88	9.17	21.49	1.07	1.56	63.0	0.5%	7.2	8.9
8	7.28	5.15	17.28	0.42	0.58	88.5	1.4%	10.3	11.1
10	8.00	3.17	12.63	0.26	0.32	95.9	1.3%	11.9	11.7
12	8.50	2.13	9.76	0.19	0.23	98.5	1.0%	12.8	11.8
Full buffer	11.11	1.14	3.35	0.11	0.18	99.5	1.1%	12.4	8.9

Table 10. *Bursty traffic performance with 1 × 2 SIMO, UMi, 10 MHz.*

With eight receive antennas, the cell spectral efficiency is significantly increased and therefore more UL overhead can be accommodated. For instance, under the UMa scenario, the number of PUCCH RBs can be increased from 4 to 18 RBs while still satisfying IMT-A requirement.

ACKNOWLEDGMENT

The authors would like to acknowledge Dr. Fan Wang and the late Dennis Schaeffer for help with this article. We dedicate this article in loving memory of our friend and colleague Dennis Schaeffer.

REFERENCES

[1] 3GPP TR 36.913, "Requirements for Further Advancements for Evolved Universal Terrestrial Radio Access (E-UTRA)," v. 8.0.1, Mar. 2009; ftp://ftp.3gpp.org

[2] A. D. Dabbagh, R. Ratasuk, and A. Ghosh, "On UMTS-LTE Physical Uplink Shared and Control Channels," *IEEE 68th VTC*, Sept. 2008.

[3] ITU-R Rep. M.2134, "Requirements Related to Technical Performance for IMT-Advanced Radio Interface(s)," 2008.

[4] NTT DoCoMo *et al*., "Prioritized Deployment Scenarios for LTE-Advanced Studies," 3GPP doc. R4-090963, RAN4, mtg. #50, Athens, Greece, Feb. 2009; ftp://ftp.3gpp.org

[5] Motorola, "DFTS-OFDM Extension for LTE-A," 3GPP doc. R1-084422, RAN1, mtg. #55, Prague, Czech Republic, Nov. 2008; ftp://ftp.3gpp.org

[6] 3GPP doc. R1-060385, "Cubic Metric in 3GPP-LTE," Denver, CO, Feb. 13–17, 2006; ftp://ftp.3gpp.org

[7] 3GPP TR 36.814, "Further Advancements for E-UTRA," v. 1.5.2, Dec. 2009; ftp://ftp.3gpp.org

[8] 3GPP TR 25.814, "Requirements for Further Advancements for Evolved Universal Terrestrial Radio Access (E-UTRA)," v. 7.1.0, Sept. 2006; ftp://ftp.3gpp.org

[9] ITU-R Rep. M.2135, "Guidelines for Evaluation of Radio Interface Technologies for IMT-Advanced," 2008.

ADDITIONAL READING

[1] B. Classon *et al*., "Overview of UMTS Air-Interface Evolution," *IEEE 64th VTC*, Sept. 2006.

[2] Motorola, "Determining a Single ACLR Value for E-UTRA UE through UL Coexistence Simulation," 3GPP doc. R4-060913, TSG RAN WG4, mtg. #40, Tallinn, Estonia, Aug. 2006; ftp://ftp.3gpp.org

[3] Motorola, "Coexistence Studies of Contiguous Aggregation Deployment Scenarios for LTE-A," 3GPP doc. R4-060913, TSG RAN WG4, mtg. #51, San Francisco, CA, May 2009; ftp://ftp.3gpp.org

BIOGRAPHIES

AMITAVA GHOSH [SM] (amitava.ghosh@motorola.com) joined Motorola in 1990 after receiving his Ph.D. in electrical engineering from Southern Methodist University, Dallas, Texas. Since joining Motorola he has worked on eight different wireless technologies starting with IS-95 and on through CDMA2000, 1xEV-DV/1XTREME, 1xEV-DO, UMTS, HSPA, 802.16e/WiMAX/802.16m, Enhanced EDGE, and 3GPP LTE. Recently, he is leading the effort from Motorola's side in defining 3GPP LTE and LTE-Advanced physical layer standards from the concept phase to the adopted baseline. He has 42 issued patents, and numerous external and internal technical papers. Currently, he is a Fellow of Technical Staff in Network Advance Technology, Motorola Networks, and works in the area of current and future air interface technologies for 802.16m, 3GPP LTE, LTE-Advanced, and other broadband technologies. His research interests are in the area of digital communications, signal processing, and wireless communications. He is an associate member of the Motorola Science Advisory Board.

RAPEEPAT RATASUK (ratasuk@motorola.com) joined Motorola in 1999 after receiving his Ph.D. in electrical engineering from Northwestern University, Evanston, Illinois. He is currently a Distinguished Member of Technical Staff in the Wireless Networks Systems and Technologies Department. He has extensive experience in 3G/4G cellular system design and analysis (LTE, HSPA, WiMAX, 1xEV-DV, W-CDMA) including algorithm development, performance analysis and validation, physical layer modeling, and simulations. He has 15 issued U.S. patents, and over 35 journal and conference papers. His research interests are in the areas of digital communications, signal processing, and wireless communications.

BISHWARUP MONDAL (bishwarup@motorola.com) received his B.E. and M.E. degrees from Jadavpur University, Calcutta, and the Indian Institute of Science, Bangalore, in 1997 and 2000, respectively, and his Ph.D. degree from the University of Texas at Austin in 2006, all in electrical engineering. Between 1997 and 2003 he worked for four years at Texas Instruments and Sasken Communication Technologies in Bangalore in the area of CAD for VLSI and audio/speech signal processing. He is presently with Motorola, Arlington Heights, Illinois. His current research interests lie in the analysis and design of multiple antenna wireless systems with quantized or partial channel information at the transmitter. He is the recipient of the 2005 IEEE Vehicular Technology Society Daniel E. Noble Fellowship.

NITIN MANGALVEDHE (nitinm@motorola.com) is a principal staff engineer at Motorola, where he has been employed since 1999 after receiving a Ph.D. in electrical engineering from Virginia Tech, Blacksburg. He worked on various wireless access technologies, including GSM/EDGE/GPRS, WCDMA, IEEE 802.11a/b/g/n, and IEEE 802.16m, for several years as part of Motorola Labs, with a focus on advanced receiver algorithms and design of next-generation wireless systems. Since 2008 he has been with the Systems and Technologies group of the Networks division, focusing on modeling, development, and performance analysis of LTE/LTE-Advanced systems. His interests are in wireless communications and digital signal processing.

TIM THOMAS (t.thomas@motorola.com) joined Motorola in 1997 after receiving a Ph.D. in electrical engineering from Purdue University. He is currently a Distinguished Member of Technical Staff in the Wireless Network Systems and Technologies Department and is working on next-generation wireless communication systems. His research interests are in channel measurement, channel estimation, MIMO communications, and adaptive antenna algorithms for mobile broadband communications.